Received: 9 September 2022 | Revised: 29 May 2023 | Accepted: 30 May 2023 | Published on: 22 June 2023

DOI: 10.1002/mrm.29765

RESEARCH ARTICLE

Magnetic Resonance in Medicine

Probing muscle recovery following downhill running using precise mapping of MRI T_2 relaxation times

Maria Holodov[1] | Irit Markus[2] | Chen Solomon[1] | Shimon Shahar[3] | Tamar Blumenfeld-Katzir[1] | Yftach Gepner[2] | Noam Ben-Eliezer[1,4,5]

[1]Department of Biomedical Engineering, Tel Aviv University, Tel Aviv, Israel

[2]Department of Epidemiology and Preventive Medicine, School of Public Health and Sylvan Adams Sports Institute, Tel-Aviv University, Tel-Aviv, Israel

[3]Center of AI and Data Science, Tel Aviv University, Tel Aviv, Israel

[4]Sagol School of Neuroscience, Tel Aviv University, Tel-Aviv, Israel

[5]Center for Advanced Imaging Innovation and Research, New York University Langone Medical Center, New York, USA

Correspondence
Noam Ben-Eliezer, Department of Biomedical Engineering, Tel Aviv University, Tel Aviv 6997801, Israel.
Email: noambe@tauex.tau.ac.il

Funding information
AFM Telethone, Trampoline grant, Grant/Award Number: 23604; Tel Aviv University Center for AI and Data Science, Grant/Award Number: 590957

Purpose: Postexercise recovery rate is a vital component of designing personalized training protocols and rehabilitation plans. Tracking exercise-induced muscle damage and recovery requires sensitive tools that can probe the muscles' state and composition noninvasively.

Methods: Twenty-four physically active males completed a running protocol consisting of a 60-min downhill run on a treadmill at −10% incline and 65% of maximal heart rate. Quantitative mapping of MRI T_2 was performed using the echo-modulation-curve algorithm before exercise, and at two time points: 1 h and 48 h after exercise.

Results: T_2 values increased by 2%–4% following exercise in the primary mover muscles and exhibited further elevation of 1% after 48 h. For the antagonist muscles, T_2 values increased only at the 48-h time point (2%–3%). Statistically significant decrease in the SD of T_2 values was found following exercise for all tested muscles after 1 h (16%–21%), indicating a short-term decrease in the heterogeneity of the muscle tissue.

Conclusion: MRI T_2 relaxation time constitutes a useful quantitative marker for microstructural muscle damage, enabling region-specific identification for short-term and long-term systemic processes, and sensitive assessment of muscle recovery following exercise-induced muscle damage. The variability in T_2 changes across different muscle groups can be attributed to their different role during downhill running, with immediate T_2 elevation occurring in primary movers, followed by delayed elevation in both primary and antagonist muscle groups, presumably due to secondary damage caused by systemic processes.

KEYWORDS
downhill running protocol, muscle recovery, qMRI, quantitative MRI, T_2, transverse relaxation time

1 | INTRODUCTION

Postexercise recovery rate is a vital component of planning training protocols and essential for maintaining high-level performance and preventing overreaching, overtraining, and injuries.[1] During recovery, while muscles strive to restore homeostasis,[2] they temporarily lose a certain level of muscle function and capacity.[3] Sufficient recovery will lead to favorable adaptations including muscle remodeling, improved function of the skeletal muscle, and enhanced performance.[2] The rate of recovery following exercise-induced muscle damage (EIMD) has been studied in relation to training experience,[4] age,[5] and gender,[6] while many studies explored efficient ways to facilitate recovery and to shed light on the individual recovery mechanisms.[7–9] These studies notwithstanding, the variability in recovery rate between and within participants remains uncertain. More in-depth and accurate tools for tracking muscle state are therefore needed to increase the sensitivity to early/pre-symptomatic muscle damage and facilitate muscle recovery after acute damage.

The severity of EIMD is influenced by training intensity,[10] duration,[11] and the type of muscle contraction (e.g., concentric, eccentric).[12] Eccentric contractions produce force by muscle lengthening,[13] causing relatively high mechanical stress on the involved structures and higher disruptions to the sarcolemma and the extracellular matrix.[14] Accordingly, eccentric protocols are used widely in studies of muscle damage and recovery.[3,15,16]

Physiologically, aerobic-based EIMD involve a cascade of microstructural processes.[16–18] During excessive eccentric contractions, high mechanical stress is placed on the involved tissues, causing myofibers tears, damage to structural proteins in the extracellular matrix, as well as to myofibrils and cell membranes. EIMD also leads to high permeability of the capillaries, osmotic shift, and leakage of muscle proteins to the blood flow.[13,19–21] Additionally, as part of the inflammatory reactions, a variety of immune cells are recruited to the site of injury, resulting in local muscle edema,[17] while phagocytic white cells such as neutrophils accumulate in the muscle as early as 1–2 h following exercise. These have a critical role in healing and removal of necrotic debris,[9] yet they can potentially trigger further cell damage by releasing oxygen free radicals, lysosomal proteases, and elastases.[22] This represents a secondary injury process, which can involve collateral damage to healthy cells that were not injured during the initial stimulation.[23]

Assessment of muscle recovery following EIMD is usually done by collecting blood markers,[24] using pain perception questionnaires,[25] and measuring stride length and force production.[16,26] MRI is another effective tool in providing region-specific assessment of muscle state, thus allowing us to identify the location of the injured area. MRI's transverse (T_2) relaxation time constant is highly sensitive to the tissues' water content, biochemistry, and microarchitecture at the cellular level. Specifically, this parameter increases as the water content increases,[27] as free water has a longer T_2 compared with bound water,[28,29] making it sensitive to microstructural changes related to EIMD.

The link between MRI measurements and postexercise cellular processes like mechanical stress, osmotic shifts, inflammation, permeability increments, edema, and secondary injury is not definitive. At the macrostructural level, however, muscle injury leads to reduction in the amount of bound water[30] and to a higher water content within the injured area,[31] thereby elevating the local T_2 relaxation time.[32] Muscle recovery aims to restore homeostasis and return to baseline fluid profile and T_2 relaxation values.[33] T_2 can therefore serve as an indirect biomarker of muscle damage and recovery.

Several studies used MRI's T_2 relaxation time as a marker for muscle damage. Aboodarda et al.[34] compared the intensity of T_2-weighted spin-echo images of the thigh before and after eccentric knee extensions, to estimate muscle damage. In studies that use quantitative T_2 values, this relaxation time is mostly estimated by fitting multi-echo spin-echo (MESE) data to the exponentially decaying signal model. For example, this method was used by Takahashi et al.[32] on subjects performing quadriceps centric contractions, by Maeo et al.[35] after downhill running (DHR), and on rats after DHR.[30,36,37] Quantitative T_2 was also used to probe muscle state in professional athletes following the completion of triathlons, using exponential curve fitting of gradient and spin-echo protocol data.[38] This protocol offers relatively short acquisition time at a tradeoff of compromised image quality and weaker encoding of the T_2 relaxation time constant.[39]

Human studies reported relatively minor changes in T_2, ranging approximately 5 ms and below in the lower limbs.[20,32,35,38] DHR studies show even smaller changes of <2 ms, which were not significant in most tested muscles.[35,38] It is therefore essential to use high-precision techniques for estimating changes in T_2 following exercise. It was previously shown that the echo modulation curve (EMC) algorithm offers high precision,[40–42] which can be used to unravel subtle pathological changes that are visually undiscernible[43,44] and allow the investigation of second-order mechanisms that affect the signal decay curves in T_2-weighted protocols (e.g., magnetization transfer and molecular diffusion).[45,46]

In this study we harness the EMC quantitative T_2 mapping technique[47] to investigate muscle recovery following intensive DHR exercise on a cohort of 24 amateur male athletes. To estimate muscle state, T_2 values

were measured at different regions in the thigh and compared across three time points: at baseline (BL; i.e., before the exercise protocol, 1 h after, and 48 h after DHR). Further investigation was performed regarding the correlation between the distribution of T_2 values and the participants' training routines and age.

2 | METHODS

2.1 | Study population

Twenty-four healthy active men volunteered to participate in the study. Participants' age and weight were 34.8 ± 9 years old and 76 ± 11 kg. All participants trained at least 4 times a week and regularly competed in long-distance running and triathlon events. Before joining the study, all participants signed an informed consent, which was approved by Shaare Zedek Medical Center (Internal Review Board #0345–19) and Tel Aviv University Ethical committee (#0000400–4) and is registered at https://clinicaltrials.gov/ (NCT04025723).

2.2 | Experimental design

Participants visited our research center on three separate occasions (Figure 1). During their initial visit (D_0), blood samples were collected. Participants also completed a health and physical activity questionnaire, a BL MRI scan, and a graded exercise test to determine maximum heart rate (HR_{max}) and volitional exhaustion (i.e., maximal O_2 consumption [VO_2max]). Subsequent visits (D_1, D_2) were scheduled 2 days apart. During D_1, a 60-min DHR protocol was performed followed by the second MRI scan, preformed 1 h after DHR. At D_2, 48 h following DHR, participants underwent the third and last MRI scan.

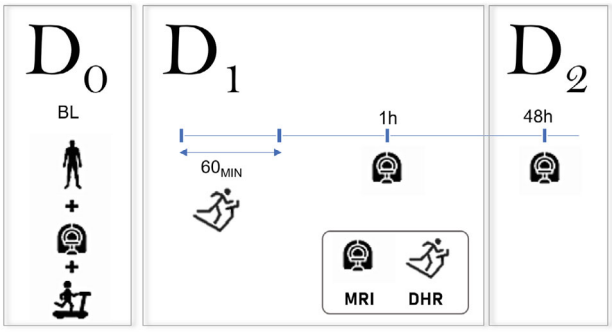

FIGURE 1 Schematic illustration of the experimental protocol. Participants arrived at three different days beginning with a screening process and an MRI scan on day zero (D_0), followed by a downhill running (DHR) exercise and additional MRI scans at subsequent visits. See Section 2 for a detailed description of the entire protocol. 1 h/48 h, 1 h/48 h after DHR protocol; BL, baseline.

Participants were instructed to refrain from consuming alcohol and caffeine for 12 h before visits, and fast for 2 hours before each visit. In addition, participants were asked to avoid unfamiliar or high-intensity exercises for 24 h before D_0, D_1 visits, and between D_1 and D_2 visits in accordance with standard exercise protocols.[48–50]

2.3 | Biochemical analysis of blood samples

Blood samples were collected at the beginning of D_0 visit in 10-mL Vacutainer tubes, and serum samples were kept at room temperature for 1 h before being centrifuged at 1300 *g* for 10 min. Samples were aliquoted into 1.8-mL microcentrifuge tubes and frozen at −80°C until analyzed. Creatine kinase and lactic dehydrogenase were subsequently estimated using a Roche clinical chemistry and immunochemistry analyzer (Cobas c111; Roche Diagnostics).

2.4 | Graded exercise test

On D_0, after MRI scan and blood test, participants underwent a graded exercise test on a motorized treadmill (Saturn 100/300, h/p/cosmos; Nussdorf-Traunstein, Germany) with an individualized protocol. During the exercise, the treadmill speed was increased every minute for the first 5–6 min until reaching a comfortable speed, at which time participants could easily run for an hour. Next, the treadmill grade was increased by 2% every minute until participants reached volitional exhaustion, defined as the point at which participants were unable to continue exercising despite verbal encouragement. During the graded protocol, breath-by-breath analysis (Quark Cardiopulmonary Exercise Testing, Cosmed) was used to collect ventilatory and metabolic measurements while the participants breathed through an oro-nasal facemask (7450 Series; Hans Rudolph). Participants' heart rate was continuously monitored using a chest strap (Garmin, model Acc; HRM-Dual). VO_2max was determined as the highest 30-s average O_2 uptake achieved during exercise, whereas HR_{max} was determined as the highest recorded HR during the test.

2.5 | DHR protocol

DHR was performed on a treadmill and consisted of a 5-min warm-up at 0% grade followed by a speed increase

every 30 s until 65% of HR_{max} was achieved. Following the warm-up, the slope of the treadmill was reduced to −10% (minus 10%) for 55 min with the running speed adjusted throughout the test so that each participant's HR remained at 65% HR_{max}. All participants completed the exercise with the target HR successfully maintained during the exercise. The average running speed was 8.9 ± 2.2 km/h.

2.6 | MRI scans

MRI scans were performed on a Magnetom Prisma 3T Siemens scanner at the imaging center of Tel Aviv University. A 6-channel receiver coil was placed on the distal quarter of the right thigh, in between the Trochanter major and the Patella, and 13 axial slices were scanned. Quantitative T_2-mapping data were collected using a 2D MESE pulse sequence for a series of increasing TE values. A long echo train (echo train length = 14) was selected, as multislice MESE protocols decay slower than the theoretical exponential decay because of stimulated and indirect echoes, which cause an elongation of T_2 relaxation curve. Experimental parameters included TR/TE = 3200/10 ms, echo spacing = 10 ms, echo train length = 14, acquisition bandwidth = 200 Hz/pixel, matrix size = 160 × 160, FOV = 220 × 220 mm^2, slice thickness = 4 mm, slice gap = 12 mm, and 2-times GRAPPA acceleration.

2.7 | MRI data processing

Figure 2 illustrates the MRI data processing pipeline. T_2 values were estimated using the EMC algorithm.[45] In this technique, a dictionary of theoretical T_2 decay curves is computed by repeating Bloch simulations of the prospective MESE protocol for a range of T_2 relaxation values and transmit-field (B_1^+) inhomogeneity levels. The resulting dictionary contains a series of signal decay curves, each associated with a unique [B_1^+, T_2] value pair. After data acquisition, the experimental signal from each voxel is matched to the dictionary of simulated curves, yielding a unique T_2 value through L_2 norm minimization between experimental and theoretical curves. All fitting procedures were programmed in house using *C++* and *MATLAB* (The MathWorks).

After all maps were calculated, image registration was performed between the three time points using *ANTS*.[51] This process used affine transformation of the T_2-weighted images from the second TE from each scan session, to track and repair the potential shifting of slices between time points along the longitudinal (z) axis of the leg.

FIGURE 2 Flowchart of the MRI data-processing pipeline. T_2 maps were generated per voxel, followed by automatic removal of fat regions. Registration was then performed between scans from different time points (D_0, D_1, D_2) followed by segmentation of specific muscles on each of the registered images. Finally, the T_2 mean value and SD were calculated for each segmented region of interest.

Manual segmentation of selected muscles was performed for each subject and at every time point on three representative slices located at the middle part of the thigh and selected by a physiologist out of the 13 slices that were scanned. Segmentation was performed on the T_2-weighted MESE images from the second TE. Two pairs of muscles were segmented: vastus lateralis (VL) and rector femoris (RF) constituting the anterior compartment of the thigh primary mover muscles, and biceps femoris (BF) and semitendinosus (ST) constituting the posterior compartment of the thigh muscles. This resulted in an overall number of 288 regions of interest (ROIs) (24 subjects × 3 slices × 4 ROIs). An experienced physiologist validated the segmentation. Finally, the mean and SD of T_2 values were calculated for each ROI, along with the corresponding number of voxels. Voxels with $T_2 > 50$ ms were tagged as not-muscle voxels and were not included in the mean and SD calculation.[52] This operation removed a few thin regions of intramuscular adipose tissue, particularly at the fascia lata.

2.8 | Statistical analysis

Statistical analysis was performed using *MATLAB* R2020b statistical toolbox. A preprocessing step was performed to test the distribution pattern of T_2 values using the Shapiro–Wilk test with a confidence level of 0.05. This step verified that the mean and SD of T_2 values were normally distributed, allowing us to use a two-tailed paired sample t-test to investigate whether they changed across time points.

Next, we tested the statistical correlation between quantitative MRI values vis-à-vis training experience, age, and weekly training routine (distance and duration). This was done using Pearson's linear correlation with $p < 0.05$ indicating statistical significance. For multiple comparisons correction, the Benjamini-Hochberg method was applied.[53,54]

3 | RESULTS

A summary of the study population characteristics, including weekly training routine and training experience, is presented in Table 1. While a wide variation existed in the weekly training duration (8 ± 4 h) and weekly accumulated running distance (47 ± 27 km), the variability of VO_2max, which constitutes the gold standard of fitness level, was relatively low (48.5 ± 6.3 mL/kg/min). Biochemical analysis of EIMD blood markers at baseline (i.e., before DHR protocol) produced 142 ± 32 U/L for lactic dehydrogenase and 224 ± 122 U/L for creatine kinase, corresponding to values at rest.[55,56]

Data for five MRI scans (3 subjects) were excluded from the analysis due to extensive motion artifacts. Remaining data points were included in the statistical analysis. An example of segmented muscles is shown in Figure 3 overlaid on a T_2-weighted axial image of the thigh (TE = 20 ms). Shaded areas denote the four selected ROIs: VL, RF, BF, and ST. Representative T_2 maps for 1 participant are shown in Figure 4 for the three time points: at baseline (BL), 1 h after, and 48 h after the DHR protocol.

Table 2 lists the mean T_2 values for each of the assayed muscles (VL, RF, BF, and ST). Statistically significant changes were found in the mean T_2 values for the primary movers (VL and RF muscles) between baseline and 1 h after DHR protocol. This change remained significant also 48 h after the exercise. Differences became significant for the other two muscles, ST and BF, at the third time point—presumably because of a secondary effect associated with a systemic response to the DHR protocol.

Analysis of intra-ROI SD of T_2 values is presented in Table 3. SD values decreased immediately following exercise for all tested muscles (BL vs. 1 h), reflecting an overall decrease in the tissue's heterogeneity. Muscle heterogeneity was also statistically different between BL and 48 h following DHR. However, there was no significant change between 1 h and 48 h after DHR, indicating that changes in tissue heterogeneity occur at short time scales and do not fully recover after 48 h. To further support these results, these analyses (of both mean and SD of T_2 values) were repeated for two other slices, producing similar results (see Supporting Information).

Baseline T_2 values from the combined ROI (containing all four muscles) were analyzed for correlation with participants' age, the number of training hours per week (3.5–20 h), weekly running distance (10–125 km), and years of experience (0.25–35 years). Statistically significant correlation was found between mean T_2 values at BL and weekly running duration ($R = -0.61$, $p = 0.003$), and between SD of T_2 values at BL and weekly running duration ($R = -0.59$, $p = 0.004$). These results remained significant after multiple comparisons correction (eight comparisons); see Supporting Information for more details. Differences in T_2 values before and after DHR were also correlated with training habits, producing no significant correlation.

TABLE 1 Characteristics of the study population.

	Mean	SD	Min	Max
Age (years)	34.8	9.0	20.0	49.0
Weight (kg)	76.0	11.0	59.0	107.0
BMI (kg/m^2)	25.0	3.0	21.0	34.0
Lean body mass (kg)	60.0	7.0	48.0	73.0
Weekly training distance (km)	47.0	27.0	10.0	125.0
Weekly training duration (h)	8.0	4.0	4.0	21.0
Training experience (years)	7.3	7.1	0.3	35.0
Maximal heart rate (bpm)	182.0	11.0	156.0	204.0
VO2 max (mL/kg/min)	48.0	6.0	31.0	63.0
Resting heart rate (bpm)	54.0	10.0	35.0	71.0

Abbreviations: BMI, body mass index; VO_2max, maximal oxygen consumption.

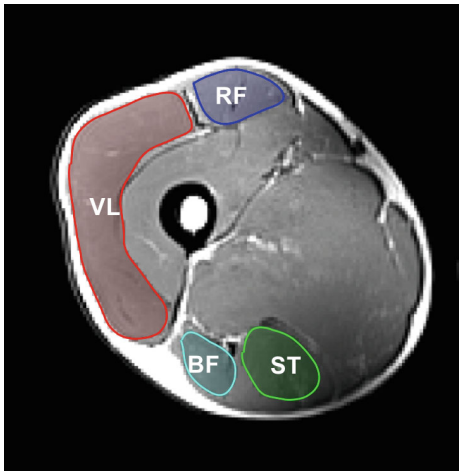

FIGURE 3 Muscle regions investigated in this study overlaid on a T_2-weighted axial image (TE = 20 ms) of the right thigh. Shaded areas correspond to vastus lateralis muscle (VL, red), rector femoris muscle (RF, blue), biceps femoris (BF, aqua), and semitendinosus (ST, green).

4 | DISCUSSION

In this study, we identified significant elevations in T_2 relaxation times alongside a reduction in the tissue heterogeneity (SD of T_2) after aerobic EIMD protocol. This reflects microstructural muscle damage and may identify

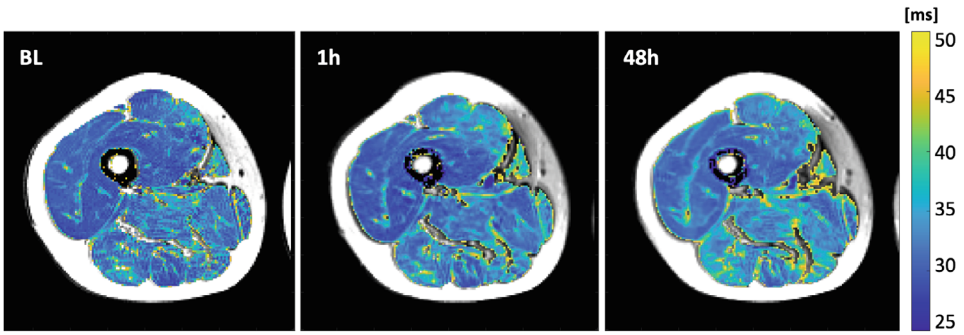

FIGURE 4 Quantitative T_2 maps of the internal thigh anatomy excluding subcutaneous fat, intramuscular adipose tissue, bone and bone marrow, and superimposed on T_2-weighted MR images. Maps are shown for three time points: baseline (BL, left), 1 hour after DHR protocol (1 h, middle), and 48 hours after DHR protocol (48 h, right).

the individual rate of recovery following EIMD. Changes in T_2 relaxation times can result from several sources including mechanical stress, inflammatory reactions, changes in cells' permeability, edema, and secondary injury. These mechanisms can be further separated into localized and systemic processes operating over different timeframes. Although mechanical stress occurs during the exercise, inflammatory reactions begin immediately after and may last for several days following stimulation.[57] Secondary injury emerges later, although the timeframe is not yet clear.[23] Based on measurements of T_2 values at three time points and across different muscle groups (agonists and antagonists), it was possible to distinguish between these short-term and long-term physiological processes.

Quantitative T_2 maps were estimated using the EMC algorithm.[45,47] By incorporating the exact scan settings and pulse-sequence timing diagram into the postprocessing procedure, this technique offers more accurate and precise mapping of T_2 values with excellent agreement to ground truth,[47] robustness to variations in T_1 relaxation times, and robustness to transmit (B_1^+) and receive (B_1^-) fields inhomogeneities.[45] This endows the EMC technique with the ability to identify subtle tissue changes, which are not detectable using conventional visual assessment of MR images[42,44] and allows us to compare different time points with high precision. Immunity to main field (B_0) inhomogeneity was also important in our study given that the same anatomy was positioned differently during each scan relative to the magnet and the receive coil.[45,58] Potential B_0 bias, however, was avoided by using a spin echo–based T_2 mapping protocol. Quantitative T_2 maps derived using standard exponential fitting might also reflect similar changes after exercise. Such values, however, will be highly overestimated[59]; suffer from higher interscanner, intrascanner, and intersubject variability[42]; and significantly lower reproducibility across scanners and scan parameters. Notably, our results were only significant on a group-wise level, which averaged out the natural interscan variability, and enables us to identify the relatively small (<2 ms) changes after DHR protocol.

A consensus exists regarding elevation of T_2 values in muscles after eccentric exercise.[21] This change is independent of the type of exercise and can last anywhere between hours and days. Maeo et al.,[35] for instance, showed significant elevations of mean T_2 24 h following DHR of 45 min at −15° slope in the vastus intermedius (+3%), lateral gastrocnemius (+6%), and soleus (+3%) muscles. Similar DHR protocols were performed on rats at −16° slope for 90 min[37] and −15° slope until exhaustion (3–4 h),[36] both reporting elevation in T_2 values for 72 h after running. Another study in humans that examined 10 repetitions of eccentric knee extension for maximum effort showed an increase of +4% in T_2 of the quadriceps muscles.[34] In contrast, a Bruce uphill treadmill protocol (a concentric exercise) led to elevation in T_2 for only about 30 min in the gastrocnemius (+14%), anterior tibialis (+10%) and soleus (+8%) muscles, after which values returned to BL.[20]

In congruence to previous findings, the current study found a significant elevation of T_2 values between BL and 1 h after DHR in the VL and RF muscles, and additional elevation between 1 and 48 h following DHR in the VL, ST, and BF muscles. We attribute the variability between different muscle groups to the different roles of the posterior and anterior muscles during DHR. In this type of exercise, the anterior muscles are the agonists (primary movers), performing eccentric contractions, whereas the posterior muscles are the antagonists undergoing concentric contraction. The immediate elevation of T_2 after exercise in the primary movers can be associated with a direct microstructural damage induced by the exercise mechanical stress. Delayed microstructural damage (i.e., secondary injury) is a slower systemic process affecting all the engaged muscles (agonists, antagonists, and synergists), which may be the source of T_2 elevation between 1 h and 48 h after the exercise time points.

A previous study that measured T_2 values in the quadriceps 48 h after DHR[35] reported an increase of 0.6 ms in the vastus medialis, 1.1 ms in the vastus intermedius, 0.3 ms in the RF, and 0.8 ms in the VL, whereas the change in the vastus intermedius was the only significant one. Another study, which measured T_2 values 3 h after a

TABLE 2 Mean ± SD of T_2 values measured at three time points and averaged across all subjects.

	Mean T_2 Values (ms)			Change Between BL and 1 h After DHR		Change Between 1 and 48 h After DHR		Change Between BL and 48 h After DHR	
z_1 slice	Baseline	1 h	48 h	Mean ± SD	*p*-Value	Mean ± SD	*p*-Value	Mean ± SD	*p*-Value
VL	30.74 ± 1.01	31.25 ± 0.84	31.64 ± 0.89	+0.53 ± 0.94	**0.0178**	+0.39 ± 0.80	**0.028**	+0.94 ± 0.75	**0.0178**
RF	30.90 ± 1.26	32.02 ± 1.13	32.34 ± 1.37	+1.20 ± 0.77	**< 0.0001**	+0.31 ± 0.74	0.056	+1.57 ± 1.04	**< 0.0001**
ST	31.61 ± 1.76	31.71 ± 1.74	32.45 ± 2.21	−0.09 ± 1.13	0.72	+0.74 ± 1.25	**0.009**	+0.45 ± 1.58	0.72
BF	32.09 ± 1.46	32.06 ± 1.67	32.91 ± 1.88	−0.11 ± 1.12	0.64	+0.85 ± 1.17	**0.002**	+0.70 ± 1.51	0.64

Note: Values are shown for four regions of interest: vastus lateralis (VL); rector femoris (RF); biceps femoris (BF); semitendinosus (ST). Also shown are the absolute differences between each of the two time points. Numbers in bold indicate statistically significant differences ($p < 0.05$) after Benjamini-Hochberg correction for multiple comparisons.

TABLE 3 Intra–region-of-interest SD of T_2 values measured at three time points and averaged across all subjects.

	SD of T_2 values (ms)			Change Between BL and 1 h After DHR		Change Between 1 and 48 h After DHR		Change Between BL and 48 h After DHR	
z_1 slice	Baseline	1 h	48 h	Mean ± SD	*p*-Value	Mean ± SD	*p*-Value	Mean ± SD	*p*-Value
VL	2.37 ± 0.51	1.98 ± 0.68	1.96 ± 0.60	−0.38 ± 0.49	**0.0017**	−0.02 ± 0.46	0.87	−0.70 ± 0.44	**0.0005**
RF	2.56 ± 0.74	1.96 ± 0.62	2.11 ± 0.75	−0.62 ± 0.65	**0.0002**	+0.15 ± 0.68	0.31	−0.42 ± 0.59	**0.003**
ST	3.60 ± 1.04	3.00 ± 1.20	3.14 ± 0.95	−0.76 ± 0.79	**0.0003**	+0.14 ± 0.60	0.27	−0.55 ± 0.83	**0.007**
BF	2.99 ± 0.84	2.45 ± 1.21	2.48 ± 0.94	−0.69 ± 0.71	**0.0002**	+0.03 ± 0.76	0.86	−0.51 ± 0.87	**0.01**

Note: Values are shown for four regions of interest: vastus lateralis (VL), rector femoris (RF), biceps femoris (BF), and semitendinosus (ST). Also shown are the absolute differences in SD values between each of the two time points. Numbers in bold indicate statistically significant differences ($p < 0.05$) after Benjamini-Hochberg correction for multiple comparisons.

triathlon,[38] reported an increase of 1.6 ms in the RF, 1.4 ms in the BF, and 0.8 ms in the ST, although no change was statistically significant. In the current study, the mean change in T_2 between BL and 48 h was 1.6 ms in the RF, 0.9 ms in the VL, 0.4 ms in the ST, and 0.7 ms in the BF. These results are consistent with the effect size measured in previous studies, although the results in the current study are statistically significant, presumably due to the high precision of the EMC technique[42,45] compared with T_2 mapping methods used in previous studies. Moreover, we are unaware of any studies that compared DHR-related muscle damage in agonist versus antagonist muscles. A related comparison was done after 3×100 repetitions of rebound jumping at the maximum speed, where T_2 elevation was observed only in the agonist muscles.[60] The current study, on the other hand, suggests that all muscles are affected, while the antagonist muscles are affected at longer time scales.

The SD of T_2 values was found to be a key marker of muscle state, reflecting the heterogeneity of the muscle tissue. In previous studies, elevation of T_2 SD values was found to correlate with neurodegenerative muscular diseases, manifesting abnormal increase of intramuscular fat and tissue fibrosis,[61–63] whereas a reduction in SD was found in lumbar intervertebral disc degeneration.[64,65] To the best of our knowledge, the current study is the first to analyze heterogeneity changes within muscle tissue following aerobic-based EIMD. Even though extensive exercise may lead to positive muscle development, it may also cause short-term microstructural damage and changes in the distribution of water molecules between subvoxel compartments, leading to changes in measured T_2 values. The current study results indicate that changes in T_2 SD were most notable between BL and 1-h time points, with no apparent change at the 48-h time point (Table 3). This reduction was significant in all tested muscles, suggesting the existence of a short-term systemic process, perhaps due to an increase in cellular permeability, which promotes the passage of large molecules from cells into the extracellular fluid. This reduces the amount of water bounds to the cells' surface and causes free water from the interstitial space to enter the cells, resulting in cell swelling.[30]

A natural variability in recovery rate exists between subjects and should be considered when designing personalized training programs. This variability is reflected in the muscles' T_2 values and depends on various parameters such as individual physiology, age, training experience, and training routine. We found no correlation between each individual factor and changes in T_2 after exercise, presumably because they need to be analyzed in tandem to accurately predict muscle performance and recovery rate. Further studies with larger sample size should also consider other cofactors such as sleep habits, dietary habits, and occupation.

4.1 | General considerations and study limitations

The present study has several aspects that should be considered. First, T_2 changes are not specific to one physiological process, and different processes may lead to similar changes in T_2 relaxation times. For example, damage to cell membrane will increase the amount of extracellular fluid and produce longer relaxation times, whereas an increase in membrane permeability due to osmotic pressure will also shift water to the extracellular space, leading to a similar elevation in T_2.

Muscle tissue is known to have multi-compartment microarchitecture, whereas specific changes in T_2 may correspond to specific subvoxel compartment (e.g., bound vs. free water or intercellular vs. intracellular changes). The use of single-component analysis may therefore be improved by using multicomponent analysis, which will deliver higher sensitivity to changes in the tissue's micro-compartmentation.[66] The current study also did not consider the effect of magnetization transfer, which can bias MESE signals. According to previous investigations, magnetization-transfer interactions accumulate along the MESE echo train, resulting in small underestimation of the calculated T_2 values.[67] These are expected to have a relatively small effect on the fast-relaxing muscle signals, although further investigation is needed to understand this effect and to incorporate it into MRI studies of muscles.

Another important aspect is the absence of a readily available and reliable tool for automatic segmentation of the individual thigh muscles,[68] which led us to perform manual segmentation. Recently, automatic neural networks have been published,[69–71] demonstrating satisfactory performance. However, none of these tools have been made publicly available, whereas in-house implementation and training require significant amounts of time and data that are beyond the scope of this study. This limited our analysis to only four muscles (two agonists and two antagonists) and three representative slices. Although a global analysis would better reflect the overall muscle state,[72] we believe that it would not produce fundamentally different results. To validate this, we reproduced all results for two additional slices (above and below the one given in Tables 2 and 3) and for a combination of all three slices, consistently producing the same findings (see Supporting Information).

The finite timeframe of the experimental design was another limiting factor. Here, we followed the recovery phase at two time points, 1 h and 48 h after DHR, due

to practical understanding that study participants belong to a population that does not rest for more than 48 h between training sessions. For this reason, participants were instructed not to exercise 24 h before a BL scan, even though 24 h may not be enough time for the muscle to stabilize after exercising. Routine workouts of the study participants were generally based on noneccentric exercise, which is more familiar, less intense, and is thus less likely to induce muscle damage.[73,74] One of the main conclusions of this observation is that future study designs should include longer rest periods before exercise.

Finally, all subjects in the current study were males. Reported findings may therefore not apply to female populations. This choice to focus on only one gender was done due to the small number of participants and the need for as homogeneous as possible group of participants. Males were chosen in this case, as they experience fewer hormonal variations, which can affect the recovery following exercise as previously reported in Oosthuyse and Bosch[75] and Enns and Tiidus.[76]

5 | CONCLUSIONS

This study shows that noninvasive measurements of MRI's T_2 relaxation time can provide quantitative information regarding muscle state and recovery following EIMD. Study findings indicate that both the mean and SD of T_2 values are useful in this context. These findings will help subsequent studies that are geared toward understanding exercise damage and recovery processes, as well as provide valuable information for planning personalized training plans, rehabilitation activities, and for understanding the pathophysiology of diseases that affect skeletal muscles.

ACKNOWLEDGMENTS

This work was supported by AFM Téléthon Grant No. 23604 and by the Tel Aviv University Center for AI and Data Science (590957).

CONFLICT OF INTEREST

Nothing to report.

ORCID

Maria Holodov https://orcid.org/0000-0002-6334-0489
Yftach Gepner https://orcid.org/0000-0002-3128-3539
Noam Ben-Eliezer https://orcid.org/0000-0003-2944-6412

REFERENCES

1. Kellmann M, Bertollo M, Bosquet L, et al. Recovery and performance in sport: consensus statement. *Int J Sports Physiol Perform.* 2018;13:240-245.
2. Peake JM. Recovery after exercise: what is the current state of play? *Curr Opin Physiol.* 2019;10:17-26.
3. Byrne C, Twist C, Eston R. Neuromuscular function after exercise-induced muscle damage. *Sports Med.* 2004;34:49-69.
4. Markus I, Constantini K, Goldstein N, et al. Age differences in recovery rate following an aerobic-based exercise protocol inducing muscle damage among amateur, male athletes. *Front Physiol*. 2022;13:916924.
5. Fell J, Williams AD. The effect of aging on skeletal-muscle recovery from exercise: possible implications for aging athletes. *J Aging Phys Act.* 2008;16:97-115.
6. Clarkson PM, Hubal MJ. Are women less susceptible to exercise-induced muscle damage? *Curr Opin Clin Nutr Metab Care.* 2001;4:527-531.
7. Shin MS, Sung YH. Effects of massage on muscular strength and proprioception after exercise-induced muscle damage. *J Strength Cond Res*. 2015;29:2255-2260.
8. Howatson G, Van Someren KA. The prevention and treatment of exercise-induced muscle damage. *Sports Med.* 2008;38:483-503.
9. Bleakley CM, Davison GW. Cryotherapy and inflammation: evidence beyond the cardinal signs. *Phys Ther Rev.* 2010;15:430-435.
10. Peake J, Wilson G, Hordern M, et al. Changes in neutrophil surface receptor expression, degranulation, and respiratory burst activity after moderate- and high-intensity exercise. *J Appl Physiol.* 2004;97:612-618.
11. Van der Meulen JH, Kuipers H, Drukker J. Relationship between exercise-induced muscle damage and enzyme release in rats. *J Appl Physiol.* 1991;71:999-1004.
12. Pokora I, Kempa K, Chrapusta SJ, Langfort J. Effects of downhill and uphill exercises of equivalent submaximal intensities on selected blood cytokine levels and blood creatine kinase activity. *Biol Sport.* 2014;31:173-178.
13. Sudo M, Ando S, Poole DC, Kano Y. Blood flow restriction prevents muscle damage but not protein synthesis signaling following eccentric contractions. *Physiol Rep.* 2015;3:1-10.
14. Hody S, Croisier JL, Bury T, Rogister B, Leprince P. Eccentric muscle contractions: risks and benefits. *Front Physiol.* 2019;10:536. doi:10.3389/fphys.2019.00536
15. LeBlanc AD, Jaweed M, Evans H. Evaluation of muscle injury using magnetic resonance imaging. *Clin J Sport Med.* 1993;3:26-30.
16. Hayashi K, Leary ME, Roy SJ, Laosiripisan J, Pasha EP, Tanaka H. Recovery from strenuous downhill running in young and older physically active adults. *Int J Sports Med.* 2019;40:696-703.
17. Markus I, Constantini K, Hoffman JR, Bartolomei S, Gepner Y. Exercise-induced muscle damage: mechanism, assessment and nutritional factors to accelerate recovery. *Eur J Appl Physiol.* 2021;121:969-992.
18. Peake JM, Suzuki K, Wilson G, et al. Exercise-induced muscle damage, plasma cytokines, and markers of neutrophil activation. *Med Sci Sports Exercise.* 2005;37:737-745.
19. Yeung EW, Ballard HJ, Bourreau JP, Allen DG. Intracellular sodium in mammalian muscle fibers after eccentric contractions. *J Appl Physiol.* 2003;94:2475-2482.
20. Varghese J, Scandling D, Joshi R, et al. Rapid assessment of quantitative T1, T2, and T2* in lower extremity muscles in response to maximal treadmill exercise Juliet. *NMR Biomed.* 2015;28:998-1008.

21. Millet GY, Tomazin K, Verges S, et al. Neuromuscular consequences of an extreme mountain ultra-marathon. *PLoS One.* 2011;6:e17059.
22. Toumi H, Best TM. The inflammatory response: friend or enemy for muscle injury? *Br J Sports Med.* 2003;37:284-286.
23. Merrick MA. Secondary injury after musculoskeletal trauma: a review and update. *J Athl Train.* 2002;37:209-217.
24. Bessa AL, Oliveira VN, Agostini GG, et al. Exercise intensity and recovery: biomarkers of injury, inflammation, and oxidative stress. *J Strength Cond Res.* 2016;30:311-319.
25. Black CD, Dobson RM. Prior eccentric exercise augments muscle pain and perception of effort during cycling exercise. *Clin J Pain.* 2013;29:443-449.
26. Vernillo G, Savoldelli A, Zignoli A, et al. Energy cost and kinematics of level, uphill and downhill running: fatigue-induced changes after a mountain ultramarathon. *J Sports Sci.* 2015;33:1998-2005.
27. Higgins CB, Herfkens R, Lipton MJ, et al. Nuclear magnetic resonance imaging of acute myocardial infarction in dogs: alterations in magnetic relaxation times. *Am J Cardiol.* 1983;52:184-188.
28. Nyman JS, Ni Q, Nicolella DP, Wang X. Measurements of mobile and bound water by nuclear magnetic resonance correlate with mechanical properties of bone. *Bone.* 2008;42:193-199.
29. Cameron IL, Ord VA, Fullerton GD. Characterization of proton NMR relaxation times in normal and pathological tissues by correlation with other tissue parameters. *Magn Reson Imaging.* 1984;2:97-106.
30. Fu C, Xia Y, Meng F, et al. MRI quantitative analysis of eccentric exercise-induced skeletal muscle injury in rats. *Acad Radiol.* 2020;27:e72-e79.
31. Archer BT, Fleckenstein JL, Bertocci LA, et al. Effect of perfusion on exercised muscle: MR imaging evaluation. *J Magn Reson Imaging.* 1992;2:407-413.
32. Takahashi H, Kuno S, Miyamoto T, et al. Changes in magnetic resonance images in human skeletal muscle after eccentric exercise. *Eur J Appl Physiol.* 1994;69:408-413.
33. Shellock FG, Fukunaga T, Mink JH, Edgerton VR. Exertional muscle injury: evaluation of concentric versus eccentric actions with serial MR imaging. *Radiology.* 1991;179:659-664.
34. Aboodarda SJ, George J, Mokhtar AH, Thompson M. Muscle strength and damage following two modes of variable resistance training. *J Sports Sci Med.* 2011;10:635-642.
35. Maeo S, Ando Y, Kanehisa H, Kawakami Y. Localization of damage in the human leg muscles induced by downhill running. *Sci Rep.* 2017;7:1-11.
36. Marqueste T, Giannesini B, Le Fur Y, Cozzone PJ, Bendahan D. Comparative MRI analysis of T2 changes associated with single and repeated bouts of downhill running leading to eccentric-induced muscle damage. *J Appl Physiol.* 2008;105:299-307.
37. Lyu X, Gao Y, Liu Q, Zhao H, Zhou H, Pan S. Exercise-induced muscle damage: multi-parametric MRI quantitative assessment. *BMC Musculoskelet Disord.* 2021;22:1-13.
38. Keller S, Yamamura J, Sedlacik J, et al. Diffusion tensor imaging combined with T2 mapping to quantify changes in the skeletal muscle associated with training and endurance exercise in competitive triathletes. *Eur Radiol.* 2020;30:2830-2842.
39. Caruthers SD, Jara H, Melhem ER. MR imaging: some applications of GRASE. *Medicamundi.* 1998;42:23-28.
40. McPhee KC, Wilman AH. Transverse relaxation and flip angle mapping: evaluation of simultaneous and independent methods using multiple spin echoes. *Magn Reson Med.* 2017;77:2057-2065. doi:10.1002/mrm.26285
41. Cosi V, Yoshimoto A, Shepherd T, Block K, Sodickson D, Ben-Eliezer N. Fast and accurate T2 mapping from multi spin echo data using Bloch-simulation-based reconstruction: investigation of intra-subject and inter-scan stability and reproducibility. In: *Proceedings of the 24th Annual Meeting of ISMRM*, Singapore City, Singapore. 2016. p. 4824.
42. Shepherd TM, Kirov II, Charlson E, et al. New rapid, accurate T2 quantification detects pathology in normal-appearing brain regions of relapsing-remitting MS patients. *NeuroImage Clin.* 2017;14:363-370.
43. Ben-Eliezer N, Raya JG, Babb JS, Youm T, Sodickson DK, Lattanzi R. A new method for cartilage evaluation in Femoroacetabular impingement using quantitative T2 magnetic resonance imaging: preliminary validation against arthroscopic findings. *Cartilage.* 2021;13:1315S-1323S. doi:10.1177/1947603519870852
44. Solomon C, Shmueli O, Shrot S, et al. Psychophysical evaluation of visual vs. computer-aided detection of brain lesions on magnetic resonance images. *J Magn Reson Imaging.* 2022. doi:10.1002/jmri.28559
45. Radunsky D, Stern N, Nassar J, Tsarfaty G, Blumenfeld-Katzir T, Ben-Eliezer N. Quantitative platform for accurate and reproducible assessment of transverse (T2) relaxation time. *NMR Biomed.* 2021;34:1-14.
46. Bnaiahu N, Omer N, Wilczynski E, Levy S, Blumenfeld-Katzir T, Ben-Eliezer N. Correcting for imaging gradients–related bias of T2 relaxation times at high-resolution MRI. *Magn Reson Med.* 2022;88:1806-1817. doi:10.1002/mrm.29319
47. Ben-Eliezer N, Sodickson DK, Block KT. Rapid and accurate T2 mapping from multi-spin-echo data using bloch-simulation-based reconstruction. *Magn Reson Med.* 2015;73:809-817.
48. Kyriakidou Y, Cooper I, Kraev I, Lange S, Elliott BT. Preliminary investigations into the effect of exercise-induced muscle damage on systemic extracellular vesicle release in trained younger and older men. *Front Physiol.* 2021;12:723931. doi:10.3389/fphys.2021.723931
49. Abaïdia AE, Lamblin J, Delecroix B, et al. Recovery from exercise-induced muscle damage: cold-water immersion versus whole-body cryotherapy. *Int J Sports Physiol Perform.* 2017;12:402-409. doi:10.1123/ijspp.2016-0186
50. Burt G, Twist C. The effects of exercise-induced muscle damage on cycling time-trial performance. *J Strength Cond Res.* 2011;25:2185-2192.
51. Avants B, Tustison N, Johnson H. Advanced normalization tools (ANTS). *Insight J.* 2009;2:1-35.
52. Azzabou N, Loureiro de Sousa P, Caldas E, Carlier PG. Validation of a generic approach to muscle water T2 determination at 3T in fat-infiltrated skeletal muscle. *J Magn Reson Imaging.* 2015;41:645-653.
53. Benjamini Y, Hochberg Y. Controlling the false discovery rate: a practical and powerful approach to multiple testing. *J R I State Dent Soc.* 1995;57:289-300.
54. Heiss R, Hotfiel T, Kellermann M, et al. Effect of compression garments on the development of edema and soreness in delayed-onset muscle soreness (DOMS). *J Sports Sci Med.* 2018;17:392-401.

55. Fallon KE, Sivyer G, Sivyer K, Dare A. The biochemistry of runners in a 1600 km ultramarathon. *Br J Sports Med.* 1999;33:264-269. doi:10.1136/bjsm.33.4.264
56. Kanther MM. Serum creatine kinase and lactate dehydrogenase changes following an eighty kilometer race. *Eur J Appl Physiol.* 1988;57:60-63.
57. Cleak MJ, Eston RG. Delayed onset muscle soreness: mechanisms and management. *J Sports Sci.* 1992;10:325-341.
58. Vaidya M, Collins C, Sodickson D, Brown R, Wiggins CG, Lattanzi RL. Dependence of B1+ and B1− field patterns of surface coils on the electrical properties of the sample and the MR operating frequency. *Magn Reson Med.* 2018;80:2256-2266.
59. Sollmann N, Weidlich D, Klupp E, et al. T2 mapping of the distal sciatic nerve in healthy subjects and patients suffering from lumbar disc herniation with nerve compression. *Magn Reson Mater Phys Biol Med*. 2020;33:713-724. doi:10.1007/s10334-020-00832-w
60. Hata J, Endo K, Tsuji O, et al. Analysis of skeletal-muscle condition after excessive loading of the lower legs by sequential magnetic resonance imaging. *J Orthop Sci.* 2019;24:873-880. doi:10.1016/j.jos.2019.01.016
61. Thibaud JL, Monnet A, Bertoldi D, Barthélémy I, Blot S, Carlier PG. Characterization of dystrophic muscle in golden retriever muscular dystrophy dogs by nuclear magnetic resonance imaging. *Neuromuscul Disord.* 2007;17:575-584.
62. Hooijmans MT, Froeling M, Koeks Z, et al. Multi-parametric MR in Becker muscular dystrophy patients. *NMR Biomed.* 2020;33:1-15.
63. Willcocks RJ, Arpan IA, Forbes SC, et al. Longitudinal measurements of MRI-T2 in boys with Duchenne muscular dystrophy: effects of age and disease progression. *Neuromuscul Disord.* 2014;24:393-401.
64. Michopoulou S, Costaridou L, Vlychou M, Speller R, Todd-Pokropek A. Texture-based quantification of lumbar intervertebral disc degeneration from conventional T2-weighted MRI. *Acta Radiol.* 2011;52:91-98.
65. Waldenberg C, Hebelka H, Brisby H, Lagerstrand KM. Differences in IVD characteristics between low back pain patients and controls associated with HIZ as revealed with quantitative MRI. *PLoS One.* 2019;14:1-14.
66. Omer N, Galun M, Stern N, Blumenfeld-Katzir T, Ben-Eliezer N. Data-driven algorithm for myelin water imaging: probing subvoxel compartmentation based on identification of spatially global tissue features. *Magn Reson Med.* 2022;87:2521-2535. doi:10.1002/mrm.29125
67. Radunsky D, Blumenfeld-Katzir T, Volovyk O, et al. Analysis of magnetization transfer (MT) influence on quantitative mapping of T2 relaxation time. *Magn Reson Med.* 2019;82:145-158.
68. Ogier AC, Hostin MA, Bellemare ME, Bendahan D. Overview of MR image segmentation strategies in neuromuscular disorders. *Front Neurol.* 2021;12:625308.
69. Guo Z, Zhang H, Chen Z, et al. Fully automated 3D segmentation of MR-imaged calf muscle compartments: neighborhood relationship enhanced fully convolutional network. *Comput Med Imaging Graph.* 2021;87:1-28. doi:10.1016/j.compmedimag.2020.101835
70. Ding J, Cao P, Chang HC, Gao Y, Chan SHS, Vardhanabhuti V. Deep learning-based thigh muscle segmentation for reproducible fat fraction quantification using fat–water decomposition MRI. *Insights Imaging.* 2020;11(1):128. doi:10.1186/s13244-020-00946-8
71. Ni R, Meyer CH, Blemker SS, Hart JM, Feng X. Automatic segmentation of all lower limb muscles from high-resolution magnetic resonance imaging using a cascaded three-dimensional deep convolutional neural network. *J Med Imaging.* 2019;6:1. doi:10.1117/1.jmi.6.4.044009
72. Amer R, Nassar J, Bendahan D, Greenspan H, Ben-Eliezer N. Automatic segmentation of muscle tissue and inter-muscular fat in thigh and calf MRI images. *International Conference on Medical Image Computing and Computer-Assisted Intervention*. Springer International Publishing; 2019:219-227. doi:10.1007/978-3-030-32245-8
73. Eston RG, Gleim G, Mchugh MP, Connolly DAJ, Eston RG, Gleim GW. Exercise-induced muscle damage and potential mechanisms for the repeated bout effect. *Sports Med.* 2014;27:157-170.
74. McHugh MP. Recent advances in the understanding of the repeated bout effect: the protective effect against muscle damage from a single bout of eccentric exercise. *Scand J Med Sci Sports.* 2003;13:88-97. doi:10.1034/j.1600-0838.2003.02477.x
75. Oosthuyse T, Bosch AN. The effect of the menstrual cycle on exercise metabolism. *Sports Med.* 2010;40:207-227.
76. Enns DL, Tiidus PM. The influence of estrogen on skeletal muscle: sex matters. *Sports Med.* 2010;40:41-58.

SUPPORTING INFORMATION

Additional supporting information may be found in the online version of the article at the publisher's website.

Appendix S1.

How to cite this article: Holodov M, Markus I, Solomon C, et al. Probing muscle recovery following downhill running using precise mapping of MRI T_2 relaxation times. *Magn Reson Med*. 2023;90:1990-2000. doi: 10.1002/mrm.29765